March 2019

Axitinib Loaded PLGA nanoparticles for Age-Related Macular Degeneration

Priya P. Narvekar
University of South Florida, narvekarpriya@ymail.com

Axitinib Loaded PLGA Nanoparticles For Age-Related Macular Degeneration

by

Priya P. Narvekar

A thesis submitted in partial fulfilment

of the requirements for the degree of

Master of Science in Pharmaceutical Nanotechnology

Department of Pharmaceutical Sciences

College of Pharmacy

University of South Florida

Co-Major Professor: Vijaykumar Sutariya, Ph.D.

Sheeba Varghese Gupta, M. Pharm, Ph.D.

Manas R. Biswal, B.F.Sc., M.F.Sc., Ph.D.

Date of Approval: 19th March, 2019

Keywords: Vascular endothelial growth factor receptor, anti-neovascularization, sustain drug release, ARPE-19, intravitreal injection

DEDICATION

This dissertation is dedicated to my parents Prakash Narhari Narvekar and Neelam Prakash Narvekar for their inspiration, love and support all their life. I will also like to remember my sister Pooja Desai for her encouragement and prayers.

ACKNOWLEDGMENTS

This thesis was possible because I could collaborate with the research team from the Lisa Muma Weitz Laboratory for Advanced Microscopy & Cell Imaging, USF Health, University of South Florida, Tampa, FL, USA for providing facility for microscopy and imaging and Department of Chemistry, College of Arts and Science, University of South Florida, Tampa, FL, USA for providing facility for DSC study.

It was an absolute privilege to have Professor Vijaykumar Sutariya as an adviser, who explained me the work going on in his lab and for giving me the opportunity to do this project under him. My sincere thanks to Professor Manas Biswal and Professor Sheeba V. Gupta for their support acceptance to my defence presentation and to spend their valuable time to read my thesis. I would also like to thank Professor Yashwant Pathak for his help and support during Masters.

I would like to offer my special thanks to Priyanka Bhatt, post-doctoral fellow in our lab who has helped me with every ups and downs during this process and finally Gulimirerouzi Fnu who is not just my helpful lab mate but an incredible friend.

TABLE OF CONTENTS

LIST OF FIGURES

ABSTRACT

Despite of all the research going on for the treatment of ocular diseases, age-related macular degeneration (AMD) remains one of the serious vision threatening disease worldwide. Choroidal neovascularization, a pathophysiological characteristic of wet AMD, is the growth of anomalous blood vessels in the eye choroidal layer. Neovascularization is a key factor in AMD and thus anti-angiogenic therapy is beneficial in reducing the development of new abnormal blood vessels to prevent progression of AMD. Axitinib, multi-receptor tyrosine kinase inhibitor, is a small molecule that works by blocking vascular endothelial growth factor receptors (VEGFR) and platelet derived growth factor receptors (PDGFR) responsible for developing neovascularization. Thus, goal of this study was to develop and characterise a sustained release formulation of Axitinib loaded poly (lactic-co-glycolic) acid (PLGA) nanoparticles. The nanoparticles were characterized for particle size and zeta potential as well as using DSC, TEM and in vitro drug release profile. The cytotoxicity of the formulation was evaluated on human retinal pigmented epithelium ARPE19 cells by MTT assay. The cellular uptake, anti-migration assay, and VEGF expression levels were found out in vitro using cells. The optimized formulation was 131.33 ± 31.20 nm in size with -4.63± 0.76 mV zeta potential. Entrapment efficiency was found to be 87.9 ± 2.7%. The cytotoxicity of ARPE19 cells was less than 12% for nanoparticles suggesting the in vitro compatibility at 10 μM concentration of drug. Cellular uptake, anti-migration assay and VEGF expression levels for the nanoparticles had greater uptake, had significant anti-angiogenic potential and exhibited inhibition of VEGF activity. The results showed successful development

of axitinib loaded PLGA nanoparticles as an alternative potential treatment option for AMD.

CHAPTER 1: INTRODUCTION

1.1 Introduction

Modern research work in the field of medicine and health focuses on better ways for drug delivery system to ensure improved therapeutic effects and reduced side effects. Among a lot research carried out on the biodegradable polymers, polylactic-co-glycolic acid (PLGA) has proved to be useful as a carrier for drug delivery and tissue engineering (1). PLGA is among the FDA approved polymers that are efficient as drug delivery vehicle due to their physical stability, biodegradability and biocompatibility. They have been intensively scrutinized as a vehicle to assist the delivery of drugs, proteins, nucleotides, and the peptides. The popularity of the PLGA nano/micro particles is also due to its ability to enhance a sustained drug delivery process, favourable deterioration abilities and the experience in the clinical field (2). Again, through control of various parameters, the physical properties of a polymer-drug complex can be adjusted to suit the appropriate dosage and release interval considering the type of the drug being dealt with. However, the toxicity associated with these require a critical analysis to enhance safety (3). Polylactic-co-glycolic acid is a copolymer of two compounds; the polylactic acid (PLA) and the polyglycolic acid (PGA). Also, the mixture contains an asymmetric α-carbon which can be described either in D and L or R and S forms. The enantiomeric forms of the compound also exist, and in general, PLGA is an acronym for the D, L- lactic-co-glycolic acid in which the D and L forms of the lactic acid live in equal proportions (4).

Axitinib is a tyrosine kinase inhibitor and works by blocking the vascular endothelial growth factor receptors (VEGFR) which in turn inhibit the activity of the endothelial growth factors. Also, it plays a crucial function in inhibiting the function of platelet-derived growth factor receptors (PDGFR) thus leading to the inhibition of neovascularization development (5). Therefore, administering axitinib intravitreally has proved to be useful in managing wet age-related macular degeneration therapy which reduces neovascularization and macular thickness thus containing the damage because of the age-related macular degeneration (6).

Age-related macular degeneration (AMD), one of the major cause for loss of vision affects many elderly patients worldwide (7). Among two types of AMD, wet-AMD is one foremost cause of vision loss and is linked to choroidal neovascularization. The acellular debris accumulates which leads to damage to macular site in retinal epithelium results into blurring of the vision (8). In response to damage in the epithelial layer, vascular endothelial growth factors (VEGF) secretion begins. Additionally due to dysfunction of ion channel and abnormal metabolism of lipid oxidative damage to cells take place (9). To pay damages for the reduce blood supply at the site, new blood vessel will start to form which will in turn increase inflammation (10, 11). Angiogenesis is an essential phenomenon of formation of new vessels in the vasculature and one of their important regulators are tyrosine kinases (12). Anti-VEGF therapy has become well known to reduce angiogenesis in cancer. Even for treatment of wet-AMD anti-VEGF therapy has gained a lot of interest to reduce neovascularization for treatment of AMD. Current therapy for AMD involves intravitreal administration of antiangiogenic agents such as Lucentis™ (Ranibizumab), Macugen® (Pegaptanib), Avastin® (Bevacizumab). However, there is rapid clearance of these agents from site of action requires frequent intravitreal instillations which increase the risk of as detachment of retina, endophthalmitis, infections, vitreous haemorrhage and increased

intraocular pressure (13) as well as reduces patient compliance. Thus, there is requirement of such delivery system which can minimize intravitreal instillation frequency of anti-angiogenic agents for efficient therapy of AMD. In the present research, axitinib loaded PLGA nanoparticles (AX-NPs) were developed and evaluated for size, zeta potential, surface morphology and in vitro drug release along with its in vitro cellular uptake and cytotoxicity. Its anti-angiogenic potential to inhibit cell migration and VEGF expression was also studies in vitro.

CHAPTER 2: MATERIALS AND METHODS

2.1 Materials

Axitinib was bought from the Selleck Chemicals, Houston, TX, USA. Poly (DL-lactide-co-glycolide) (PLGA, Mw 15000 Da) containing lactide/glycolide ratio of 50:50 was acquired from the Acros Organics (NJ, USA). Polyvinyl alcohol, Mw 100000, was purchased from the Fisher Scientific (USA). Both the Coumarin 6 dye and the Dialysis membrane, Mw 10000, was outsourced from Sigma Aldrich (St. Louis, MO). Fetal Bovine Serum and penicillin-streptomycin (10000 U/ml) were purchased from Gibco Thermo Fisher Scientific, USA. 3-(4,5-dimethylthiazol-2-yr)-2,5-diphenyltetrazolium bromide salt (MTT reagent), and nucleus stain DAPI (4′,6-diamidino-2-phenylindole) both of which were outsourced from the Tocris Bioscience (MN, USA). Cell maskTM deep red plasma stain was obtained from Thermo Fisher Scientific, (USA). BCA protein assay kit and Invitrogen™ eBioscience™. Human VEGF-A Platinum ELISA Kit were purchased from Fisher scientific branch in USA. ARPE-19, a human retinal pigment epithelial cell line (ATCC® CRL2302™) and Dulbecco's Modification of Eagle's Medium F 12 (DMEM F12) was obtained from American Type Culture Collection (ATCC) (VA, USA). Cell culture Phosphate Buffer Saline (1X) (PBS) was obtained from Corning Cellgro (Manassas, VA). Trypsin (0.05%) was purchased from Thermo Fisher (Lansing, MI). All the analytical reagent used were analytical grade and hence no further purification was needed.

2.2 Cell Culture

All the cell line studies were performed onthe human retinal epithelial cell line, ARPE-19 (ATCC CRL2302™). DMEM F12 medium supplemented with 10% v/v FBS and 1% 10000 u/ml penicillin-streptomycin antibiotics were used for the maintenance of cells. The cells were incubated in a humidified atmosphere at 5% CO_2 at 37 °C.

2.3 Preparation of Axitinib Loaded PLGA NPs

AX-NPs were prepared by the o/w solvent evaporation method (2). The drug and the polymer were dissolved in a 2 ml of DMSO: acetone (1:9 vol/vol) at a weight ratio of 1:7 at room temperature. The resultant solution was then slowly added into 1% w/v PVA solution using 23G syringe while in constant stirring at 700 rpm at room temperature (RT). After that, the organic solvent was allowed to evaporate at RT, and the resulting volume of the aqueous dispersion was collected. The suspension was then centrifuged at 5000 rpm for 5 mins at RT so that the unentrapped drug can be removed. Further the supernatant was centrifuged at 18000 rpm at 4 ºC for about 2 h to allow nanoparticles to settle down. After being centrifuged, pelleted nanoparticles were washed using distilled water and collected (2). In the same manner, blank nanoparticles excluding the drug and Coumarin 6 loaded nanoparticles were formulated. Figure 1 shows the graphical presentation of the preparation method of AX-NPs.

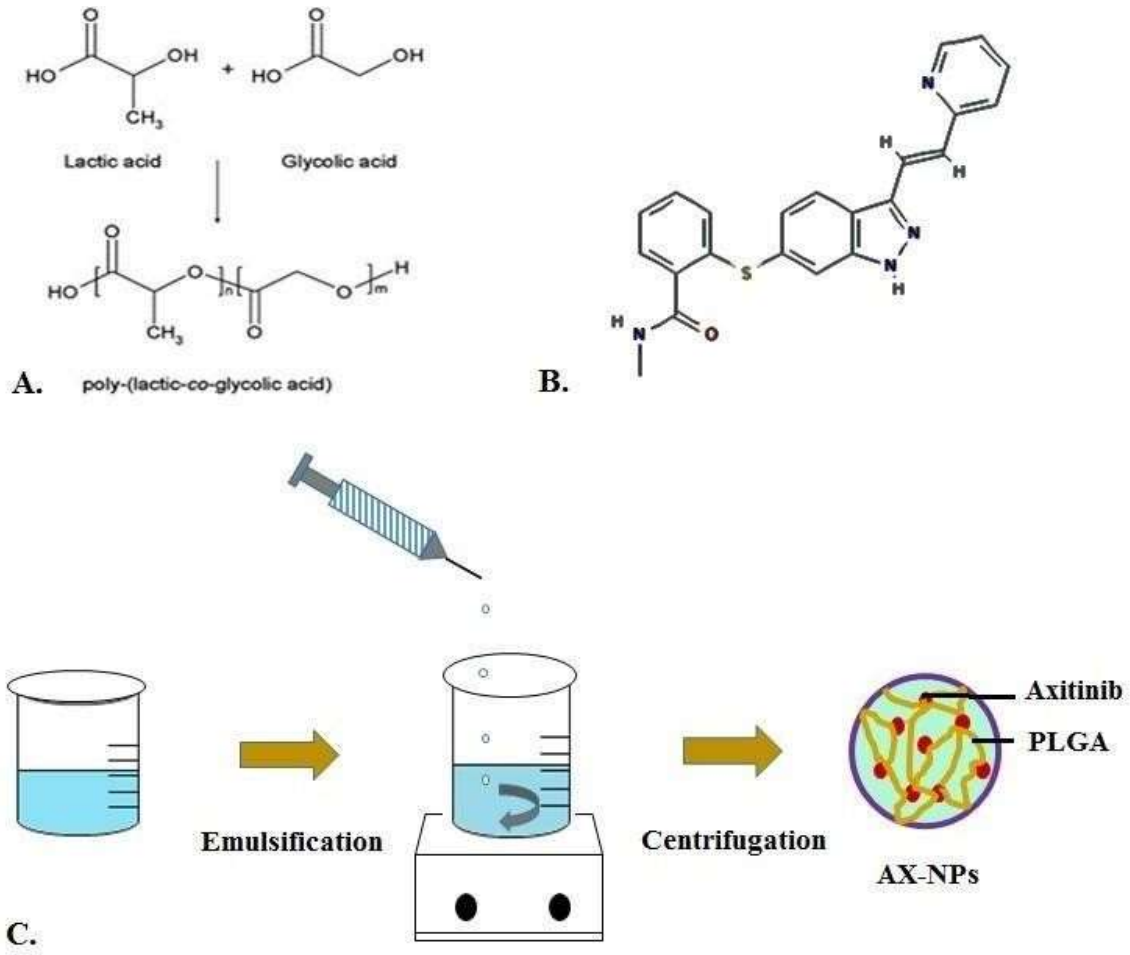

Figure 1: (A) Structure of PLGA with its monomers, (B) Structure of the axitinib drug, (C) Graphical representation of method of preparation of AX-NPs.

2.4 Differential Scanning Calorimetry

The analyses of the sample using the differential scanning calorimetry were conducted on the DSC- Q 20 (TA Instruments, New Castle, DE USA, Q series Q20-2288-DSC software). Blank aluminium pan was used as a reference (14). About 4mg of the sample powders were then heated form a temperature of about 30 to 300 ºC at a rate of 10°C min^{-1} under the nitrogen purge (50 mL/min) (15). The procedure was carried out in both the thermal analysis involving pure axitinib drug, the physical mixture of axitinib and the PLGA nanoparticles, polymer and lastly on

the axitinib loaded PLGA nanoparticles.

2.5 Particle Size and The Zeta Potential

Through the aid of a laser dynamic light scattering (DLS), the mean particle sizes of AX-NPs were determined. This investigation was carried out within a measuring angle of about 90 º at a temperature of approximately 25 ºC using a sample, adequately diluted with filtered distilled water (16). For every sample analysed, the mean diameter and the standard deviation of five readings were determined through the application of the multimodal analysis. The outcome ofthe analysis was then reported in triplicates. The results of zeta potential were obtained along with polydispersity index (PDI).

Zeta potential of nanoparticles was determined based on Smoluchowski equation that considers electrophoretic mobility of the nanoparticles and their back-scatter at 90° (17). The analysis was carried out in triplicate after ten times dilution of nanoparticles using double distilled water using zeta cuvette and Zeta Sizer Nano ZS 90 (Malvern Instruments Ltd., UK, Zeta Sizer Software Ver. 7.10)

2.6 Transmission Electron Microscopy

Transmission Electrode Microscope (TEM) (JEOL JEM 1400 electron microscope with Gaton camera, Peabody, MA, USA), was used to study the morphology, size and shape of AX-NPs. This involved placing the sample on the EMS formvar support film square grid, 200 Cu. It

was then allowed to air dry approximately for 5 to 10 minutes. It was further treated with 2% w/v phosphotungstic acid for negative staining. The investigation was conducted at an accelerating voltage of about 120 kV with 40000 magnifications.

2.7 Entrapment Efficiency

AX-NPs were first centrifuged at 5000 rpm for 10 mins to remove the unentrapped drug from the suspension. Then the collected supernatant containing NPs was further centrifuged at 18000 rpm for 20 min to collect AX-NPs pellet. The pellet was washed thrice with DI water to separate the traces of unentrapped drug from the surface and collected. Analysis was done using UV spectrophotometer at a wavelength of 260 nm (λmax) in methanol as a solvent. The contents of the AX drug were then determined from the UV curve produced. Hence the AX entrapment efficiency and the loading efficiency were calculated through using below equations.

$$\% \text{ Entrapment efficiency} = \frac{\text{Actual amount of drug loaded in nanoparticles}}{\text{Actual amount of drug used for preparation}} \times 100$$

$$\% \text{ Loading efficiency} = \frac{\text{Amount of AX in nanoparticles}}{\text{Total amount of nanoparticles}} \times 100$$

2.8 In Vitro Drug Release Study

The in vitro drug release study of axitinib solution in DMSO and AX-NPs was carried out using dialysis bag (MWCO 10000 Da) diffusion technique (18). The dialysis tube was immersed in 20 ml of release medium (Phosphate buffer saline with pH 7.4) containing 0.1% (v/v) Tween

80. Using a magnetic stirrer, the contents were continuously stirred at 150 rpm and the temperature was adjusted to 37 ^{0}C. At predetermined intervals of 0.25, 0.5, 1, 2, 3, 4, 5, 6, 12, 24, 48, 72, 96, 120, 144 and 168 hrs., 1 ml of sample was removed and replaced with the fresh release media. Drug concentration was determined by using the UV spectrophotometry at a wavelength of 260 nm after dilution of the sample with methanol.

2.9 Cytotoxicity Study

The MTT assay was initiated to help determine the level of cytotoxicity associated with the AX-NPs comparing it with the pure drug solution, in ARPE-19 cell line (human retinal pigment epithelial cells). The cells were cultured at a suitable density of 5000 cells/well in a 96 well plate in 200 µl of DMEM supplemented with 10% FBS. The incubation was carried out at a temperature of about 37 °C with access to 5% atmosphere CO_2 for 24 h to enable proper attachment and assist in the growth of the cells (19). Both the formulations involving the nanoparticles and the pure drug solution were subjected to dilution using as serum-free DMEM F12 medium to come up with varied concentrations of axitinib drug. After 24 h culture, the cells were treated with prepared formulations and the treatment was kept for 4 hours. At the end of the incubation period, the treatment was removed, and cells were washed once using sterile 1X PBS. The procedure was then followed by the addition of fresh complete DMEM F12 medium containing 10% FBS for period of 24 to 48 h. After specified time, 100 µl of MTT reagent (1 mg/mL) solution was added to each well and the cells were incubated in same condition as previous for 4 h (17). The medium in each plate was then replaced with 100 µl of dimethyl-sulfoxide and intensity of the colour of the dissolved formazan crystals was measured using microtiter plate

reader at wavelength 595 nm. Cells treated with DMEM F12 acted as the negative control while the ones treated with 0.1% Triton X were the positive control in the experiment. Cell viability was given relative to that of the negative control (20)

2.10 Cellular Uptake

To determine the cell uptake potential of the AX-NPs, confocal microscopy was carried out. Prepared formulations like blank nano-formulation, drug formulation and coumarin formulations were prepared. The cells were seeded in the density of $2x10^5$ per well in a six well plate. The plate in the incubated to achieve 70% confluency. The cells was washed thrice with PBS. The wells were then treated with the prepared coumarin loaded nanoparticles and blank nanoparticle as a reference. The six well plate was then incubated with all the prepared nano-formulations for the period of 4 hrs. The plate is then subsequently washed thrice with PBS and then fixed with 4% paraformaldehyde. DAPI was used as a nuclear staining followed by Cell-mask ™ deep red staining for membrane staining. This is then examined under confocal microscope FV1200 (Olympus, Tokyo, Japan) at 60x magnification.

2.11 Wound Scratch Assay

Wound healing assay procedure was carried out to assist in the analysis of the inhibitory effect of axitinib and its formulation on VEGF induced angiogenesis. Human retinal pigment epithelial cells were grown in twenty-four well plates and allowed to reach 80% confluency. The wounds were then developed with much care using pipette tip. The average size of the wounds

developed was measured and found to be around 300µm. for the sake of the study, wound width within 5% variation was considered. The wounds were then cleaned with sterile PBS two times eliminate partly adhered cells on the plates due to the wound. These wells were then subjected to treatment using the serial dilution of drug formulation and Nanoparticulate formulation in incomplete media at 1µM and 10µM concentration (21).

Cell migration was analysed under the microscope and quantified through obtaining the measurements of the area covered by the cells that had migrated from the wound edges using Image software. To inspect the effect VEGF on the cell migration, two wells were also kept at high two concentrations and treated with VEGF simultaneously. Thus, one well consisted of a complete medium while the other one was treated with VEFG to act as reference and controls in that order. Incubation was done still at the average body temperature of about 37 °C in a CO2 incubator (5%) for 48 hrs. The treatments were removed after incubation, and the cells were washed with PBS three times, fixed using 70% ethanol. Images were then obtained, and the wound width was measured using images captured by the microscope. The width of the untreated group at 0 h was considered 100% and relatively % recovery of the wound was compared.

2.12 Anti-VEGF ELISA

Human retinal pigment epithelial cells were cultured in twenty-four well plates at the density of 5 x 10^4 cells/mL and allowed to become confluent. The day of the examination, the culture media was replaced with incomplete media and subjected to treatment. The treatment group consisted of a free drug solution and axitinib-NPs, each at 10µM concentration and were further incubated for a total period of 72 hours (22). Quantification of the secreted VEGF in the culture

media was done by ELISA method using Human VEGF-A Platinum ELISA Kit following manufacturer's instructions. The protein content in the cells was estimated using Pierce BCA protein assay kit after collecting cell lysate and the by normalizing VEGF secretion to total protein. Samples were read using ELISA plate reader at 450 nm absorbance, and 550 nm and the difference were recorded, followed by calculating inhibition of VEGF secretion using standard curve.

2.13 Statistical Analysis

The results obtained were presented as mean and the standard deviation and the investigation conducted with the aid of students t-test. The variance in the lipid profile was investigated statistically using a one-way analysis of variance followed by turkey's test. The probability values od $p<0.05$ were statistically significant.

CHAPTER 3: RESULTS AND DISCUSSIONS

3.1 Differential Scanning Calorimetry

Pure AX drug, physical mixture of PLGA and AX as well as AX-NPs were studied for physicochemical characterization using differential scanning calorimetry (DSC) technique. Figure 2 demonstrates DSC thermal analysis of AX, physical mixture of AX and PLGA and AX-NPs (15), (13), (27). The physical state of drug molecule in NPs affects their release and solubility in external medium and so DSC thermograms is helpful in identifying the nature or physical state of drug alone and while being loaded in NPs (28). AX showed sharp endothermic peak at around 212 ^{0}C indicating its specific melting point.

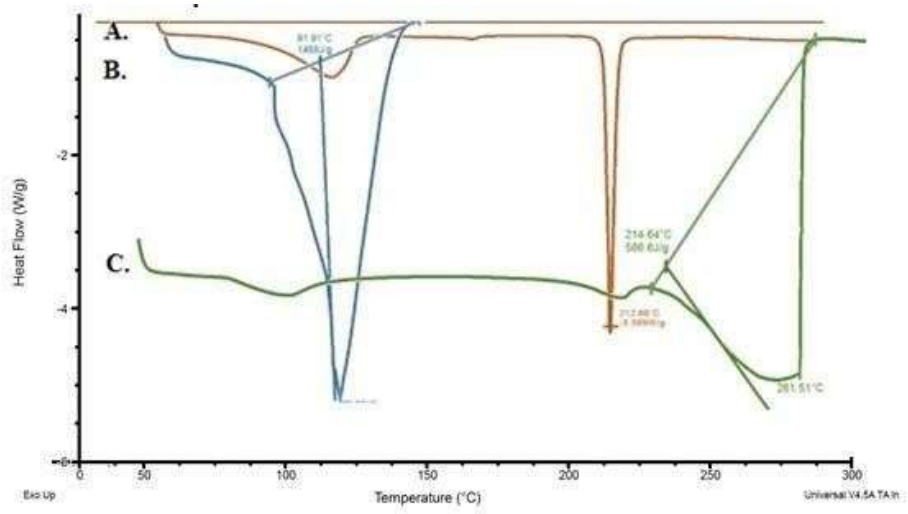

Figure 2: DSC spectra of (A) AX pure drug, (B) AX-NPs formulation and (C) AX and PLGA physical mixture.

This endothermic peak was not present in DSC spectra of AX-NPs approving the complete loading of AX in NPs and confirming amorphous form of loaded AX. Incompatibility between the polymer and drug can also be determined from DSC thermograms from the alterations in the transition temperature of individual components that generates added peaks in thermogram (23). Thus, DSC study also disclosed the compatibility of the AX and PLGA.

3.2 Particle Size and Zeta Potential

The size of AX-NPs was measured using DLS technique and was found to be 131.33 ± 31.20 nm with PDI of 0.108 ± 0.005. The mean zeta potential of AX-NPs was determined using a Malvern Zetasizer Nano ZS90 and was found to be -4.63± 0.76 mV. Figure 3(A) shows Z-average for the particle size for AX-NPs (24). It has been observed that with increased concentration of PLGA at drug to PLGA weight ratio of 1:10, the axitinib entrapment was not increased significantly however an increase in the PLGA concentration resulted in increased viscosity of the organic phase thus the diffusional resistance of drug particles from the organic phases to the aqueous phase was increased. This led to increase in the particle sizes of particles (data not shown). Thus, 1:7 weight ratio was optimised for preparation of AX-NPs. The zeta potential affects the stability of the nanoparticles both extremes significantly either in the positive side or the negative side leads to higher repulsive forces being witnessed. The repulsive forces existing between similar electric charge blocks and hence they enhance the ease of dispersion. For the combined dynamic and steric stabilization, minimum zeta potential is recommended. Formulation involving the use of non-ionic surfactants exhibited average zeta potential whereas the formulations without the use of surfactant demonstrated a higher zeta potential. This scenario depicted could be due to the

existence of carbonyl groups within the extremes of the polymeric chains of pure PLGA nanoparticles (25).

3.3 Transmission Electron Microscopy

TEM revealed that the particle size of AX-NPs was around 110 nm. Though this was in disagreement with that of particle size obtained by dynamic light scattering, such difference can be easily realized as DLS reports the hydrodynamic diameter of the particles whereas in TEM analysis the size obtained was of the particle fixed in grid. TEM images (figure 3 (B)) confirmed nanoparticles of uniform size and were in concurrence with the DLS results and were spherical with smooth surface. TEM was used to confirm the information that the nanoparticles were spherical and was not in aggregate.

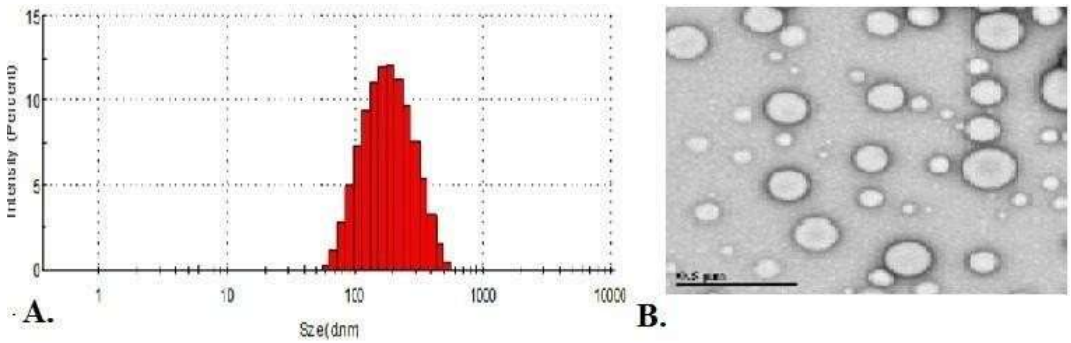

Figure 3: A. Z-average of AX-NPs, B. TEM image of AX-NPs with 40,000X magnification at accelerating voltage of 120 kV (scale bar 0.5 µM).

3.4 Entrapment Efficiency

Encapsulation efficiency was calculated by centrifuging the NP solution and resuspending the NP pellet in methanol. Entrapment efficiency was found 87.9 ± 2.7%. Percent

drug loading was found to be around 11%. UV spectroscopy was used to determine the encapsulation efficiency of AX by comparing the absorbance in methanol to standard dilutions of AX in methanol (r^2=0.9994) at λ_{max} of 260 nm. Three weight ratios (1:5, 1:7, 1:10) of AX:PLGA were studied to see the effect of polymer concentration on entrapment and loading of the drug in NPs. Out of which 1:7 was optimised as significant increase in entrapment efficiency was observed compared to weight ratio of 1:5. However there was no significant change in entrapment efficiency was observed for weight ratio of 1:10 (optimization data not shown).

3.5 In Vitro Drug Release Study

The in-vitro release study of AX from drug solution and AX-NPs were carried out by dialysis method. To mimic the in vivo eye posterior area environment, phosphate buffer saline having pH of 7.4 was used a release media and the study was performed at 37 °C. Tween-80 (0.1% v/v) was added to the release medium to improve the solubility of drug in release medium as well as to maintain the sink condition. The release profile of AX from solution as well as NPs have been shown in figure 4 for the period of 7 days.

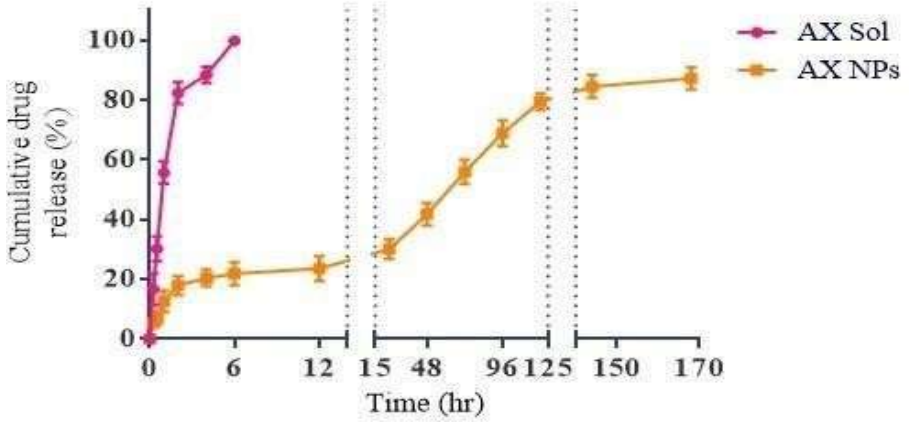

Figure 4: Cumulative drug release of AX from AX solution and AX-NPs up to 7 days at 37 °C in phosphate buffer saline at pH 7.4, (mean ± SD, n =3).

The release of AX from solution was rapid and almost 100% of AX was released within 6 h in release medium. While the AX-NPs initially demonstrated burst release of 18.4±2.2 % of AX within first hour which may be because of the adhered drug to the outer surface of NPs. But, after that AX-NPs exhibited sustained release profile ox AX with 23.7±1.4% release at the end of 24 h followed by 84.2±4.1% at the end of seven days (26).

3.6 Cytotoxicity Study

The cytotoxicity of the AX drug solution and AX-NPs was studied using the MTT assay in the human retinal pigmented epithelium cell line ARPE-19.

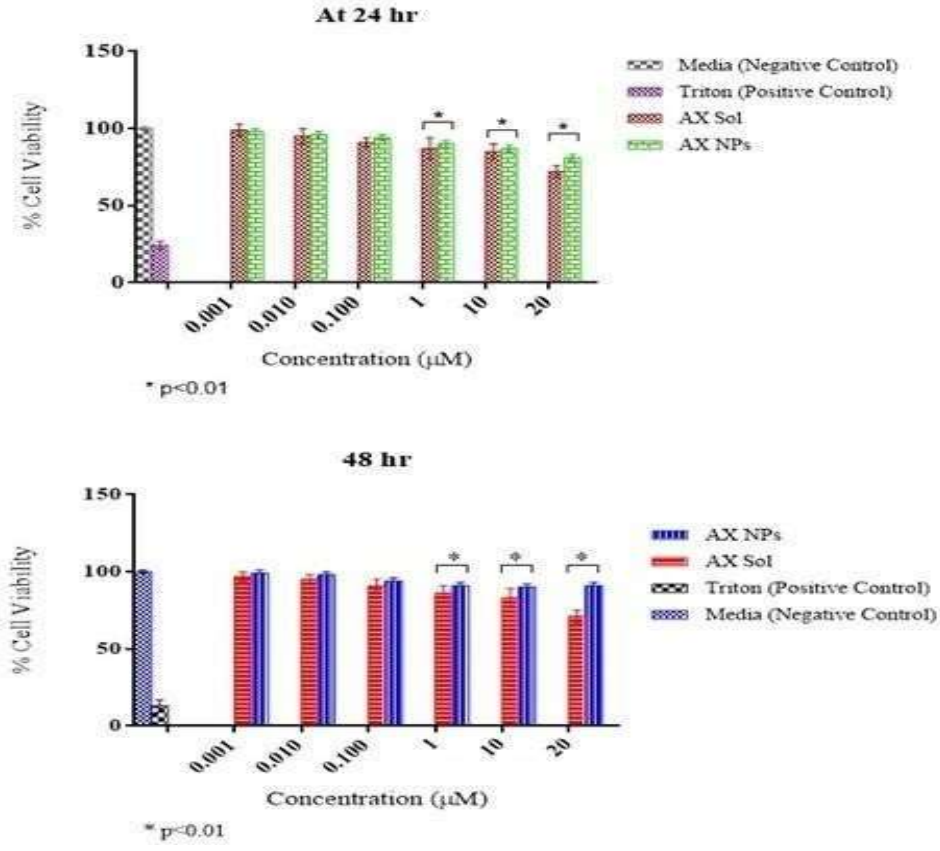

Figure 5: % cell viability at different concentrations of AX drug solution and AX-NPs at (A) 24 h and (B) 48 h in ARPE 19 cell line, (mean ± *SD*, n =3).

Cells were treated in serum-free medium with various concentrations (0.001, 0.01, 0.1, 1, 10 and 20 μM) of AX in solution as well as NPs in triplicates for 24 and 48 h. To study the cytotoxic potential of polymer alone, blank PLGA NPs were also evaluated for MTT assay. The resulting cell viability was compared to that of the control untreated cells, which was established as 100%. Results specified that the viability of cells was higher than 90% for AX-NPs at 10 μM and 20 μM concentration tested for both the time points tested whereas, for drug solution viability at 20 μM was found to be 78% and 63% respectively for 24 h and 48 h, thus demonstrating non-toxic nature of NPs (figure 5). The biocompatible and biodegradable nature of PLGA has been demonstrated so far and thus FDA has approved use of PLGA based on its safety profile. Data from MTT assay also supported its biocompatible nature with ARPE-19 cells.

3.7 Cellular Uptake

Coumarin-6 loaded PLGA NPs were evaluated for cellular uptake upon incubation with ARPE-19 cells at 37 °C. Coumarin-6 is a hydrophobic fluorescent dye which mimics hydrophobic nature of AX and was used to locate the nanoparticles and their uptake in to the cells. Figure 6 shows confocal images demonstration the uptake of coumarin 6-loaded PLGA NPs into ARPE 19 cells at various time points at 37 °C. The left first panel shows nucleus stained with nucleus staining dye DAPI with blue fluorescence. The next panel is representing presence of cells as red fluorescence is because of the stained cell membrane with Cell Mask Deep Red stain. In the third panel from the left, uptake of coumarin-6 loaded NPs was observed and showing green fluorescence in the cytoplasm of the cells which confirms presence of NPs in

cell cytoplasm and the last panel demonstrating the merged images of all. The blank in the figure is untreated cells which were kept as control. The intensity of green fluorescence depicting uptake of NPs in cells has been observed to increase with increase in treatment time. This may be because of the fact that the uptakeof NPs follows receptor mediated endocytosis process and with increase in the treatment time more NPs can bind with the VEGFR present on the ARPE-19 cells leads to enhanced cellular uptake.

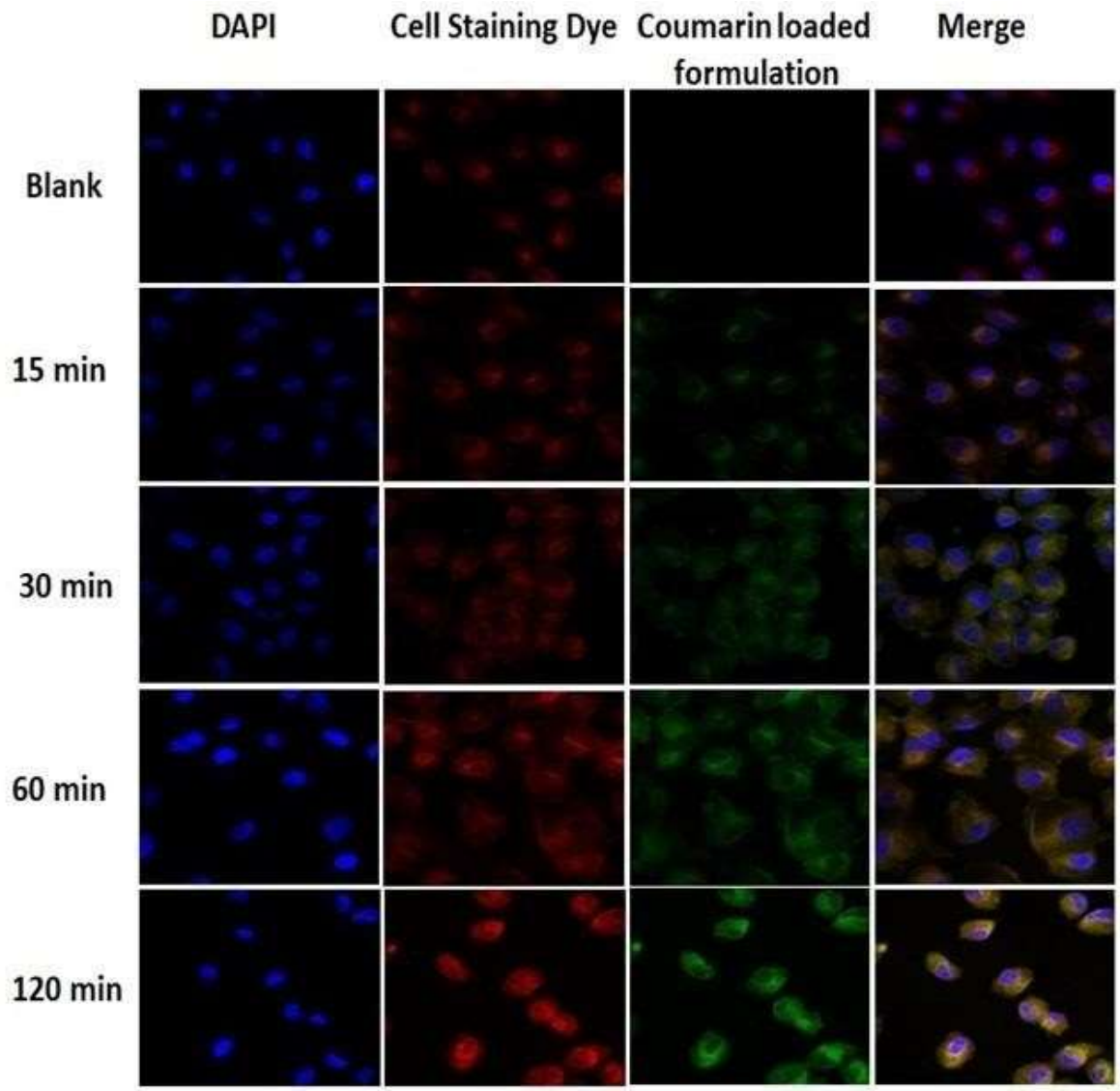

Figure 6: Cellular uptake of coumarin 6-loaded PLGA NPs in ARPE-19 cells at various time points at 37 °C.

3.8 Wound Scratch Assay

Wound scratch assay was performed to study migration of the cell which is one of the primary stages that leads to angiogenesis. The evaluation of the cell locomotion avails a significant estimation of inhibition of cell growth through conducting appropriate measurement on wound recovery under microscopic evaluation (27).

The cells were imaged immediately after making a wound served as a reference while the untreated group demonstrating covering of wound naturally served as a control. Figure 7(A) demonstrates microscopic images showing recovery of wound after treatment of cells with AX solution and AX-NPs in presence and absence of angiogenesis promoting agent (100 nM of VEGF165, rhVEGF; R&D Systems). Fig. 7 (B) shows the % wound recovery for respective images in quantifying graphical plot. Concentration dependent inhibition of wound recovery was observed ($p < 0.01$); least for the group with maximum concentration of AX in NPs (10 μM). The 100 nM of VEGF165 (rhVEGF; R&D Systems) increased the migration of cells to greatest extent and hence wound recovery as seen in fig. 7 (A). However, co-treatment of AX-NPs formulation with VEGF165 could resist the action of VEGF165 as well as inhibited VEGF-induced angiogenic manifestations in ARPE-19 cells and did not significantly improved the cell migration based wound recovery. These results indicate that AX-NPs efficiently and selectively inhibits VEGF-induced angiogenesis in ARPE-19 cells.

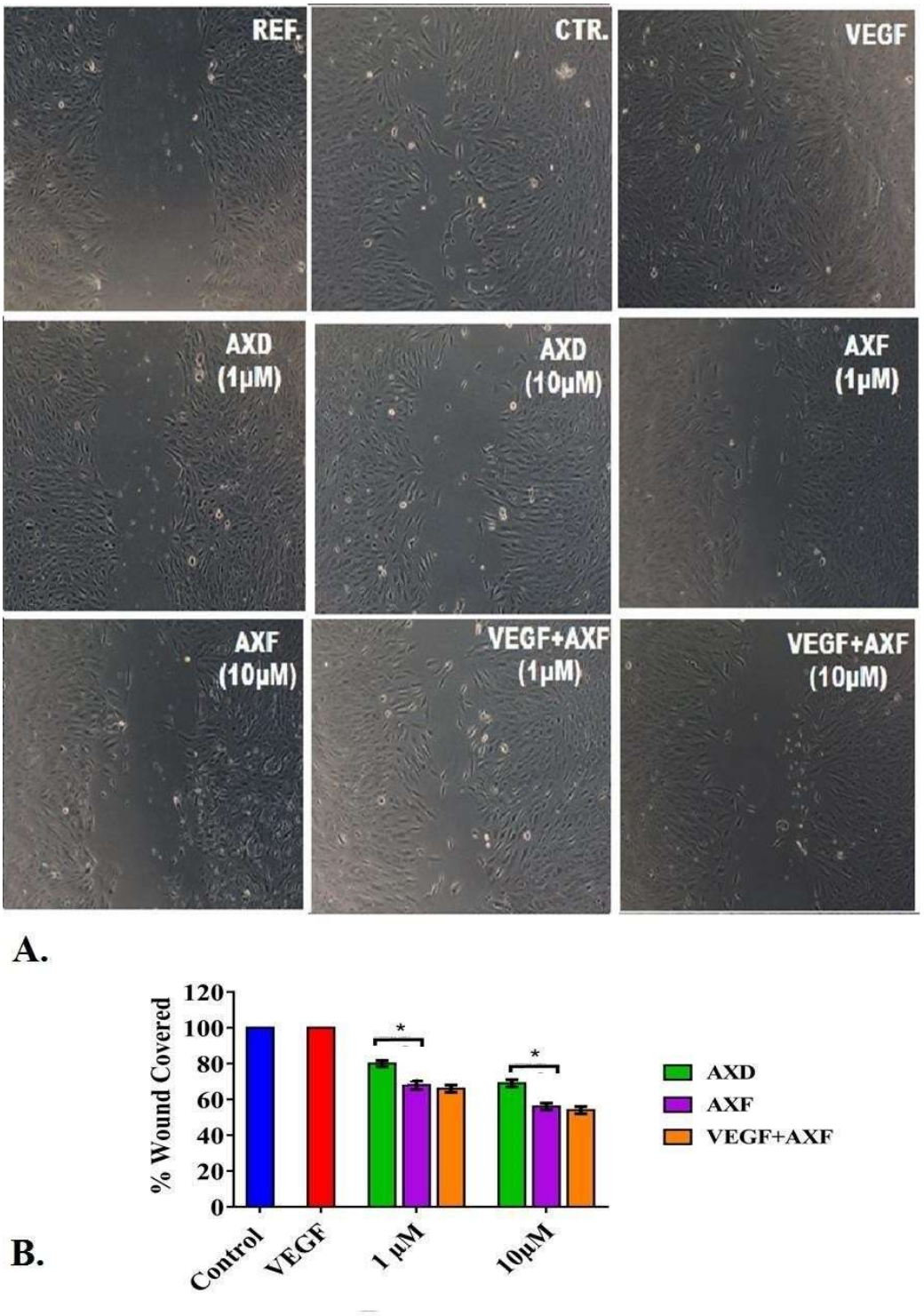

Figure 7: (A) Wound scratch assay images for ARPE-19 cells treated pure AX drug solution (AXD), various concentration of AX-NPs (AXF) in presence and absence of VEGF 165. (B) Percent wound covered after 48 h in comparison to control for AXD and AXF at various concentrations in presence and absence of VEGF 165, *$P < 0.01$ vs control, (mean ± *SD*, n=3).

3.9 Anti-VEGF ELISA

The effect of the AX drug solution and AX-NPs on secretion of VEGF was studied using Anti-VEGF ELISA in ARPE-19 cells. Samples were collected after 12, 24, 48 and 72 hours of treatment and the amount of VEGF-A was measured using the Human VEGF-A Elisa kit. % VEGF secretion values are demonstrated using the control group value as 100% (Figure 8). VEGF secretion was noticeably reduced by the free AX solution throughout all treatment groups. AX-NPs have similar effects on VEGF-A secretion. ELISA results showed significantly ($P < 0.05$) decreased VEGF protein levels after exposure to AX-NPs (10 µM equivalent of AX) in ARPE19 at 24, 48, and 72 h in comparison with control cells and cells treated with drug solution.

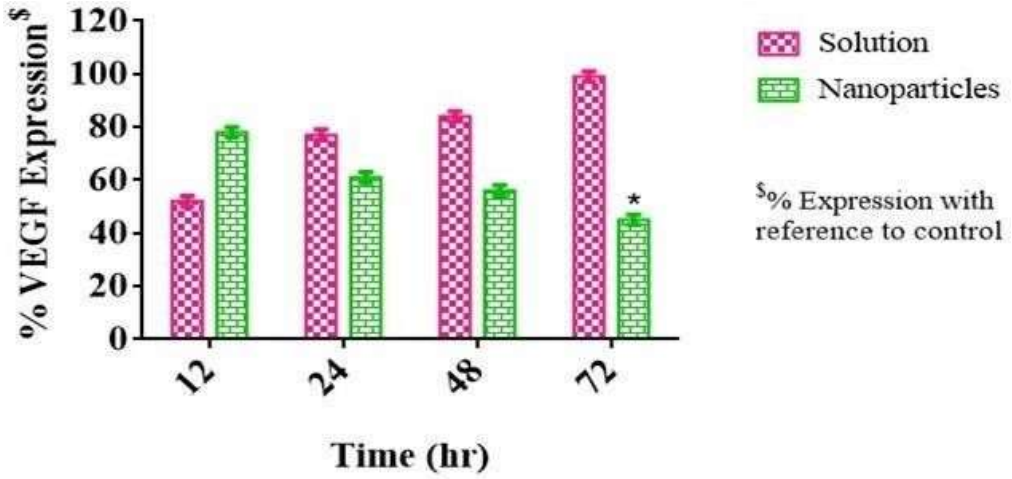

Figure 8: % VEGF expression in ARPE-19 cells treated with AX drug solution and AX-NPs for different time point determined using ELISA assay method (mean ± *SD*, n =3).

The observation depicted could be because of an initial high level of free drug available within the cells in case of employment of the solution form of the medicine since the correlation of the scenario with the release profile of the formulation is hard to be determined. However, in case of nanoparticle formulation, there was an initial low level of VEGF control which at later time points became stronger as the drug released from the matrix over a longer duration (28), (29).

Therefore, an end to note is the excellent sustained inhibitory effect of nanoparticle formulation as compared to drug solution was observed.

CHAPTER 4: CONCLUSION

The AX-NPs was successfully developed, characterized and tested in vitro in human retinal epithelial ARPE-19 cells manifesting its effectiveness in the wet AMD. The formulation may present an important approach of treating wet-AMD due to its capability in ensuring a sustained release of drug and potential in inhibiting VEGF expression which in the clinical field is of great importance. It is therefore considered more superior as compared other oral formulations that portray low efficacy with more side effects. The intravitreal installation of the prepared nanoparticles can be conducted for efficient local delivery of the drug into the posterior segment of the eye, hence a sustained release formulation may be of great importance that reduces the frequent administration of intravitreal injection. Thus, this is an attractive approach that can be further investigated in vivo and in clinical setting to demonstrate its application for wet AMD therapy.

REFERENCES

1. Kelly SJ, Hirani A, Shahidadpury V, Solanki A, Halasz K, Varghese Gupta S, et al. Aflibercept Nanoformulation Inhibits VEGF Expression in Ocular In Vitro Model: A Preliminary Report. Biomedicines. 2018 Sep 11;6(3). PubMed PMID: 30208574. Pubmed Central PMCID: PMC6165497. Epub 2018/09/14. eng.
2. Patel J, Amrutiya J, Bhatt P, Javia A, Jain M, Misra A. Targeted delivery of monoclonal antibody conjugated docetaxel loaded PLGA nanoparticles into EGFR overexpressed lung tumour cells. Journal of microencapsulation. 2018 Mar;35(2):204-17. PubMed PMID: 29542378. Epub 2018/03/16. eng.
3. Wadhwa A, Mathura V, Lewis S. Emerging novel nanopharmaceuticals for drug delivery2018. 35 p.
4. Danhier F, Ansorena E, Silva JM, Coco R, Le Breton A, Préat V. PLGA-based nanoparticles: An overview of biomedical applications. Journal of Controlled Release. 2012 2012/07/20/;161(2):505-22.
5. Atkins M, Joseph R, Ho T, Vaishampayan U, Ali S, Matrana M, et al. Abstract B201: A phase 1 dose-finding study of X4P-001 (an oral CXCR4 inhibitor) and axitinib in patients with advanced renal cell carcinoma (RCC). Molecular Cancer Therapeutics. 2018;17(1 Supplement):B201-B.
6. Mandal A, Pal D, Agrahari V, Trinh HM, Joseph M, Mitra AK. Ocular delivery of proteins and peptides: Challenges and novel formulation approaches. Advanced drug delivery reviews. 2018 Feb 15;126:67-95. PubMed PMID: 29339145. Pubmed Central PMCID: PMC5995646. Epub 2018/01/18. eng.
7. Pennington KL, DeAngelis MMJE, vision. Epidemiology of age-related macular degeneration (AMD): associations with cardiovascular disease phenotypes and lipid factors. 2016;3(1):34.
8. Nowak JZJPR. Age-related macular degeneration (AMD): pathogenesis and therapy. 2006;58(3):353.
9. Al Gwairi O, Thach L, Zheng W, Osman N, Little PJJJoo. Cellular and molecular pathology of age-related macular degeneration: potential role for proteoglycans. 2016;2016.
10. Jager RD, Mieler WF, Miller JWJNEJoM. Age-related macular degeneration. 2008;358(24):2606-17.
11. Nickla DL, Wallman JJPir, research e. The multifunctional choroid. 2010;29(2):144-68.
12. Vhora I, Patil S, Bhatt P, Gandhi R, Baradia D, Misra A. Receptor-targeted drug delivery: current perspective and challenges. Therapeutic delivery. 2014;5(9):1007-24. PubMed PMID: 25375343. Epub 2014/11/07. eng.
13. Del Amo EM, Rimpelä A-K, Heikkinen E, Kari OK, Ramsay E, Lajunen T, et al. Pharmacokinetic aspects of retinal drug delivery. 2017;57:134-85.
14. Patil S, Bhatt P, Lalani R, Amrutiya J, Vhora I, Kolte A, et al. Low molecular weight chitosan–protamine conjugate for siRNA delivery with enhanced stability and transfection efficiency. RSC Advances. 2016;6(112):110951-63.

15. Bhatt P, Lalani R, Vhora I, Patil S, Amrutiya J, Misra A, et al. Liposomes encapsulating native and cyclodextrin enclosed paclitaxel: Enhanced loading efficiency and its pharmacokinetic evaluation. International Journal of Pharmaceutics. 2018 2018/01/30/;536(1):95-107.
16. Yewale C, Baradia D, Patil S, Bhatt P, Amrutiya J, Gandhi R, et al. Docetaxel loaded immunonanoparticles delivery in EGFR overexpressed breast carcinoma cells. Journal of Drug Delivery Science and Technology. 2018 2018/06/01/;45:334-45.
17. Patil S, Lalani R, Bhatt P, Vhora I, Patel V, Patel H, et al. Hydroxyethyl substituted linear polyethylenimine for safe and efficient delivery of siRNA therapeutics. RSC Advances. 2018;8(62):35461-73.
18. Hemal Tandel PB, Keerti Jain, Aliasgar Shahiwala, Ambikanandan Misra. In-Vitro and In-Vivo Tools in Emerging Drug Delivery Scenario: Challenges and Updates. In: Misra ASaA, editor. In-Vitro and In-Vivo Tools in Drug Delivery Research for Optimum Clinical Outcomes: CRC Press; 2018.
19. Shahiwala A, Misra A. In-Vitro and In-Vivo Tools in Drug Delivery Research for Optimum Clinical Outcomes2018.
20. Rini BI, Melichar B, Fishman MN, Oya M, Pithavala YK, Chen Y, et al. Axitinib dose titration: analyses of exposure, blood pressure and clinical response from a randomized phase II study in metastatic renal cell carcinoma. Annals of oncology : official journal of the European Society for Medical Oncology. 2015 Jul;26(7):1372-7. PubMed PMID: 25701454. Epub 2015/02/24. eng.
21. Bhatt P, Lalani R, Mashru R, Misra A. Abstract 2065: Anti-FSHR antibody Fab' fragment conjugated immunoliposomes loaded with cyclodextrin-paclitaxel complex for improved in vitro efficacy on ovarian cancer cells. Cancer Research. 2016;76(14 Supplement):2065-.
22. Caceres C, Canfarotta F, Chianella I, Pereira E, Moczko E, Esen C, et al. Does size matter? Study of performance of pseudo-ELISAs based on molecularly imprinted polymer nanoparticles prepared for analytes of different sizes. The Analyst. 2016 Feb 21;141(4):1405-12. PubMed PMID: 26796951. Epub 2016/01/23. eng.
23. Carvalho DdM, Takeuchi KP, Geraldine RM, Moura CJd, Torres MCL. Production, solubility and antioxidant activity of curcumin nanosuspension. Food Science and Technology. 2015;35:115-9.
24. Bhattacharjee S. DLS and zeta potential - What they are and what they are not? Journal of controlled release : official journal of the Controlled Release Society. 2016 Aug 10;235:337-51. PubMed PMID: 27297779. Epub 2016/06/15. eng.
25. Forest V, Cottier M, Pourchez J. Electrostatic interactions favor the binding of positive nanoparticles on cells: A reductive theory. Nano Today. 2015 2015/12/01/;10(6):677-80.
26. Dhule SS, Penfornis P, Frazier T, Walker R, Feldman J, Tan G, et al. Curcumin-loaded gamma-cyclodextrin liposomal nanoparticles as delivery vehicles for osteosarcoma. Nanomedicine : nanotechnology, biology, and medicine. 2012 May;8(4):440-51. PubMed PMID: 21839055. Pubmed Central PMCID: PMC4943321. Epub 2011/08/16. eng.
27. Wang X, Ji Z, Chang CH, Zhang H, Wang M, Liao YP, et al. Use of coated silver nanoparticles to understand the relationship of particle dissolution and bioavailability to cell and lung toxicological potential. Small (Weinheim an der Bergstrasse, Germany). 2014 Jan 29;10(2):385-98. PubMed PMID: 24039004. Pubmed Central PMCID: PMC4001734. Epub 2013/09/17. eng.
28. Halasz K, Kelly SJ, Iqbal MT, Pathak Y, Sutariya V. Utilization of Apatinib-Loaded

Nanoparticles for the Treatment of Ocular Neovascularization. Current drug delivery. 2019;16(2):153-63. PubMed PMID: 30332959. Epub 2018/10/20. eng.
29. Fornaguera C, Dols-Perez A, Caldero G, Garcia-Celma MJ, Camarasa J, Solans C. PLGA nanoparticles prepared by nano-emulsion templating using low-energy methods as efficient nanocarriers for drug delivery across the blood-brain barrier. Journal of controlled release: official journal of the Controlled Release Society. 2015 Aug 10;211:134-43. PubMed PMID: 26057857. Epub 2015/06/10. eng.